^{1,2,3}H, ^{4}He emission from ^{96}Ru nuclei ($E^* \simeq 113$ MeV): Test for transmission coefficients in the evaporation model

M. Kildir,* G. La Rana, R. Moro, A. Brondi, A. D'Onofrio, E. Perillo, V. Roca, M. Romano, and F. Terrasi
Dipartimento di Scienze Fisiche dell'Università and Istituto Nazionale di Fisica Nucleare, Pad. 20 Mostra d'Oltremare, 80125 Napoli, Italy

G. Nebbia and G. Viesti
Istituto Nazionale di Fisica Nucleare and Dipartimento di Fisica dell'Università di Padova, I-35131 Padova, Italy

G. Prete
Istituto Nazionale di Fisica Nucleare, Laboratori Nazionali di Legnaro, I-36020 Legnaro, Padova, Italy
(Received 26 December 1991)

A detailed comparison between measured energy spectra and cross sections of ^{1,2,3}H and ^{4}He, evaporated from the composite system ^{96}Ru ($E^* \simeq 113$ MeV), and the predictions of the statistical model, has been carried out. Results obtained with transmission coefficients derived from optical model (OM), ingoing-wave boundary-condition model (IWBCM) and fusion systematics (FS) are presented. The best overall description of the data is obtained using IWBCM transmission coefficients, with reduced s-wave barriers, including, in the level density, deformations slightly larger than those predicted by the rotating liquid drop model (RLDM). ^{2,3}H yields are well reproduced by IWBCM transmission coefficients, while they are largely overestimated by the OM ones; the failure is found to be related to the imaginary part of the optical potential which accounts for the absorption of nonfusion reactions, in peripheral collisions. No combination of phase space and transmission coefficients is able to reproduce, simultaneously, the low emission barrier and the cross section observed for protons.

PACS number(s): 25.70.Gh, 25.70.Jj

I. INTRODUCTION

Evaporative light charged particles have proved to be a powerful probe for the investigation of many aspects related to the properties of hot rotating nuclei ($E^* < 100$ MeV) [1–8]. The presence of spin-induced deformations appears to be well established for many composite systems [2–4] on the basis of the comparison of particle energy spectra and angular distributions with the predictions of the evaporation model. The time of the shape relaxation of the emitting nucleus has been found to be also important in the evaporation process [5].

Besides deformations,the existence of novel features of the nuclear surface along the formation of the composite system has been suggested for some composite systems [6–8]. In particular, the measured emission barriers for ^{1,2}H and ^{4}He, not reproduced by the evaporation model, would reflect the formation of an hot diffuse nuclear surface. This picture is confirmed by self-consistent Hartree-Fock calculations of hot nuclear density [9].

The interpretation of barrier lowering in the statistical model is not free from controversies [10–12] which arise from the use of different evaporative codes adopting different parametrizations of the level density and different sets of transmission coefficients. Among a number of fundamental open questions concerning the use of the statistical model, the choice of the transmission coefficients is particularly important. In fact, they play a leading role in the determination of the extent of the nuclear deformation and, according to recent papers [6–8], in the investigation on possible dynamical effects responsible for barrier reductions. Emphasizing that the transmission coefficients are related to the inverse process cross section, i.e., fusion, McMahan and Alexander [13] have analyzed fusion excitation functions for protons and alpha particles in order to determine the appropriate transmission coefficients. As pointed out in Ref. [12], for the system 120-MeV ^{30}Si+^{30}Si, transmission coefficients derived from fusion systematics [14] produce alpha energy spectra harder than those obtained from optical model transmission coefficients. An important contribution to this subject is given in a recent paper [15] where the ingoing-wave boundary-condition model (IWBCM) and optical model (OM) transmission coefficients are compared. The authors pointed out that the special effects of the imaginary part of the optical potential, responsible for transparency, shape resonances, and peripheral absorption, can be misleading in the context of the evaporation model, as they include nonfusion reactions in the inverse process. In this framework recent experimental data [16,17] have indicated that the evaporation model

*Permanent address: Middle East Technical University, Ankara, Turkey.

systematically overestimates the deuteron and triton yields at high excitation energy ($\simeq 100-400$ MeV) if OM transmission coefficients are used. The failure of the model is attributed to the large percentage of nonfusion reactions accounted for by the OM transmission coefficients [17].

We report here a detailed comparison between measured energy spectra and cross sections of ^{1,2,3}H and ^{4}He emitted from the composite system ^{96}Ru [$E^* \simeq 113$ MeV, $J_{max} \simeq 69\hbar$ [4]] formed in the reaction 180-MeV ^{32}S+^{64}Ni, with the predictions of the evaporation model. The major objective is to illustrate the results obtained with different sets of transmission coefficients, having strong experimental constraints to the model such as energy spectra and cross sections of all the light charged particles. Particular emphasis is given to the following two aspects strictly related to the transmission coefficients. The first one concerns deuteron and triton yields, which appear to by systematically overpredicted, using OM transmission coefficients. The second one is related to the need of barrier lowering in the statistical model.

^{4}He emission from the same nucleus at different excitation energies ($E_x = 82.2-115.7$ MeV) has been studied in Ref. [4], where OM transmission coefficients have been used in the analysis. It has been found that ^{4}He energy spectra can be reproduced, enhancing the level density, indicating the onset of deformations at high spins. In spite of this, alpha particle cross sections at higher excitation energies are systematically underestimated by the model.

II. EXPERIMENTAL PROCEDURES

The experiment was carried out at the XTU Tandem of the Laboratori Nazionali di Legnaro (Padova), using a 180-MeV beam of ^{32}S with an average current of $\simeq 50$ electrical nA. A self-supporting target of ^{64}Ni 500 μg/cm^2 thick, 96% isotopically enriched, has been used. Spectra of protons, deutrons, tritons, and alpha particles were measured by four silicon tritelescopes (50 μm,500 μm,5000 μm) at laboratory angles $\theta_{lab} = 20°$, 30°, 45°, 60°, 125°, and 135°. The telescopes at the most forward angles (20° and 30°) were protected from the elastic scattering by a gold foil 40 mg/cm^2 thick. At the other angles, 10-mg/cm^2 gold foils were used, in order to shield the detectors from low-energy electrons and photons. Solid angles were determined by geometric measurements (2.0 msr at 20°, 30°, and 45°; 1.9 msr at 60°; 4.4 msr at 125° and 135°). The energy calibration was performed by normalizing a precision pulser to the peak due to the 5.48-MeV ^{4}He-particle decay of ^{241}Am.

Experimental ^{1,2,3}H and ^{4}He angular distributions in the center-of-mass (c.m.) system are shown in Fig. 1. The differential cross sections have been determined by numerical integration of the energy spectra, taking as lower limit the same energy threshold. The evaporative process from the composite system dominates at backward angles ($\theta_{lab} > 50°$, corresponding to $\langle \theta_{c.m.} \rangle > 70°$), where the angular distribution becomes isotropic, while the presence of a nonevaporative component is observed at forward

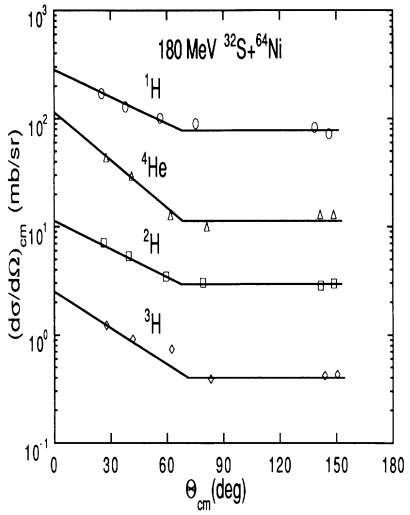

FIG. 1. Measured ^{1,2,3}H and ^{4}He angular distributions in the c.m. system for the reaction 180-MeV ^{32}S+^{64}Ni. The symbols are experimental data, and the lines have been drawn to guide the eye.

angles. At backward angles the contribution of other sources such as deep inelastic fragments or fission fragments has been estimated to be negligible as indicated by a Monte Carlo simulation of such processes using the code GANES [18]. The calculation shows that a significant contribution of these processes would provide a shape of the energy spectra very different from that observed experimentally. Furthermore, a comparison of the shape of the energy spectra in the c.m. system shows that it does not depend on the angle, confirming the evaporative nature of the spectra at backward angles. A similar result has been found in Ref. [4], where the same composite system has been studied.

Evaporative particle total cross sections have been obtained assuming an isotropic angular distribution normalized to the angle corresponding to 60° in the laboratory system, whose spectrum was not affected by energy cuts in the center-of-mass system, for all particles. Variations up to 15% in the cross sections are obtained, assuming different shapes of the angular distribution, with anisotropies up to 2. The spectrum at $\theta_{lab} = 60°$ has been used for comparison with the evaporation model.

III. COMPARISON WITH CASCADE PREDICTIONS

Measured ^{1,2,3}H and ^{4}H energy spectra and cross sections have been compared with the predictions of the evaporation model for the composite system ^{96}Ru ($E^* \simeq 113$ MeV). Calculations have been performed with the code CASCADE [19].

As pointed out in Ref. [4], fission is an important decay channel for the composite system under study. Experimental fission data for the system ^{35}Cl+^{62}Ni, close to our system, are available in Ref. [20]. The authors found that a significant reduction (FFB=0.54) in the rotating liquid drop model (RLDM) [21] fission barrier and an increase in the level density at the saddle point ($a_f/a_\nu = 1.04$),

compared with that of the rotating ground state, are required to reproduce the experimental data. These fission parameters provided a constraint to our calculations, as was done in the data analysis in Ref. [4].

A. Energy spectra

^{1,2,3}H and ^{4}He energy spectra in the center-of-mass system, corresponding to $\theta_{lab}=60°$, are compared with CASCADE calculations in Fig. 2. This version of the code allows one to calculate energy spectra in the c.m. system, rather than the channel energy distributions, as in the original version. The calculated spectra have been normalized to the maximum of the experimental ones in order to compare the shapes. The sets of parameters shown in Table I have been employed. Set 1 represents the default values used by the code; set 2 corresponds to the best fit to the alpha particle spectrum, modeling the phase space and including fission parameters according to Ref. [20]. The severe constraints provided by the shape of the ^{4}He energy spectrum allowed us to determine a unique set of parameters. The two sets of parameters produce $\sigma_{fiss}=108$ and 341 mb, respectively. The second value is much closer to the interpolated value of the fission excitation function measured for the system ^{35}Cl+^{62}Ni in Ref. [20]. In both calculations optical model transmission coefficients [22–26] have been used. The yrast lines corresponding to sets 1 and 2 are shown in Fig. 3, where the vertical line marks fission cutoff angular momentum. The ratio of major to minor axis of the nucleus, according to the RLDM, is also shown as a function of the angular momentum. Such deformations correspond to the yrast line labeled by set 1, while the yrast line labeled by set 2 corresponds to deformations slightly larger.

As can be seen in Fig. 2, set 1 is far from reproducing the shapes of the spectra of all four particles. In particular, the measured energy spectra are significantly softer than the calculated ones. While for tritons the low-energy side is almost reproduced, deviations appear for

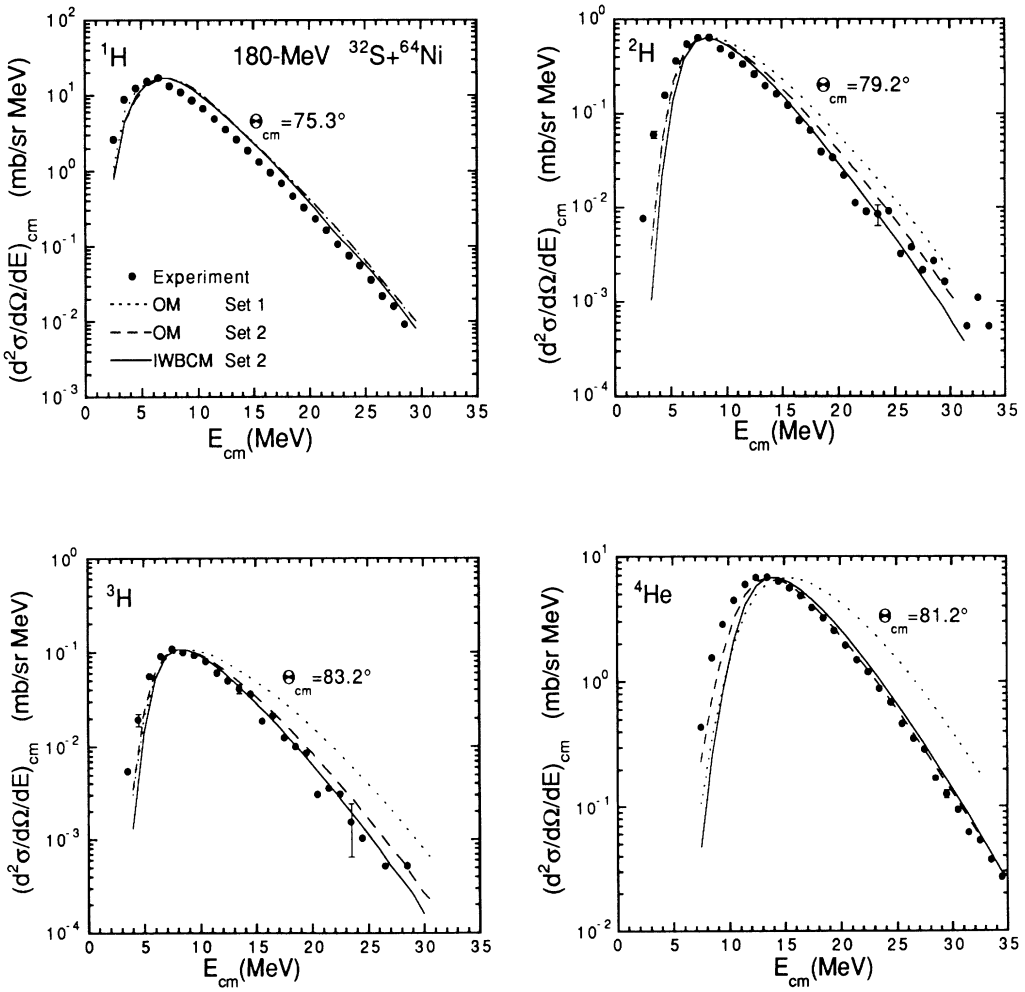

FIG. 2. Comparison between ^{1,2,3}H and ^{4}He experimental energy spectra and CASCADE calculations, performed with optical model (OM) and ingoing-wave boundary-condition model (IWBCM) transmission coefficients. Sets 1 and 2 of parameters are given in Table I.

TABLE I. Parameters of evaporation calculations using CASCADE code for $^{32}S + ^{64}Ni$.

Angular momentum distribution in the compound nucleus:
(1) $J_{crit} = 69\hbar$,
(2) diffuseness $\Delta = 2\hbar$.
Myers-Swiatecki liquid drop mass formula [29].
Level density parameters at low excitation ($E^* < 10$ MeV):
(1) Fermi gas level density formula with parameters from Dilg *et al.* [30];
(2) effective moment of inertia, $\zeta = 0.85\zeta_{rigid}$.
Level density parameters at high excitation:
set 1, ($E^* > 20$ MeV); set 2, ($E^* > 15$ MeV).
(1) Fermi gas level density formula [31] with parameters from LDM [32].
(2) Level density parameter,
set 1, $a_{LDM} = A/8$; set 2, $a_{LDM} = A/8.5$.
Yrast line:
(1) Moment of inertia for rigid body with radius parameter:
set 1, $r_0 = 1.23$ fm; set 2, $r_0 = 1.28$ fm.
(2) Deformability parameters (DEF and DEFS) used to calculate the effective moment of inertia as a function of angular momentum:
set 1, DEF $= 4.7 \times 10^{-6}$, DEFS $= 1.2 \times 10^{-8}$;
set 2, DEF $= 9.1 \times 10^{-5}$, DEFS $= 9.7 \times 10^{-10}$.
Fission:
(1) Level density parameter at the saddle point:
set 1, $a_f = A/8$; set 2, $a_f = A/8.17$.
(2) Fraction of the liquid drop barrier FFB:
set 1, FFB $= 1.0$; set 2, FFB $= 0.54$.
Transmission coefficients for emitted particles calculated by
(A) optical model (OM) potential,
(1) neutrons, Wilmore and Hodgson [22],
(2) protons, Perey [23],
(3) deuterons, Lohr and Naeberly [24],
(4) tritons, Becchetti and Greenlees [25],
(5) alpha particles, Huizenga and Igo [26];
(B) ingoing-wave boundary-condition model (IWBCM), which uses real part of the optical model potential given above [27];
(C) Fusion Systematics (FS), which uses the Hill-Wheeler expression [28] and fusion *s*-wave barriers [14].

protons, deuterons, and alpha particles. Using set 2, good agreement is obtained for the alpha particles and a substantial improvement for ^{2,3}H at the high-energy side. The quality of the agreement for the ^{4}He spectrum is essentially the same as that found in Ref. [4] for the same system. For protons, the two calculations provide, as expected, essentially the same shape of the spectrum with the results shifted to a higher energy of about 1 MeV. As far as the low-energy side is concerned, no substantial changes are obtained for all the particles going from set 1 to set 2.

A modified version [27] of the program TL, included in the CASCADE package, has been used to generate transmission coefficients according to the IWBCM, as input for CASCADE, for all the nuclei involved in the evaporative chain. Center-of-mass energy ranges of 32 MeV for n, ^{1,2,3}H, and ^{4}He in steps of 1 MeV and for orbital angular momenta up to $32\hbar$ have been considered. The same real part of the potential used in the OM transmission coefficients has been adopted. Using these transmission coefficients with all the other parameters of set 2, the high-energy sides of the deuteron and triton energy spectra are better reproduced, while a significant disagreement is obtained for the alpha particles at the low-energy

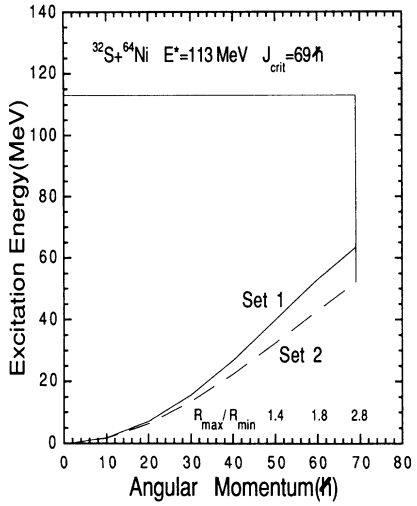

FIG. 3. Yrast plot for ^{96}Ru. Yrast lines have been calculated using sets 1 and 2 of parameters given in Table I. The vertical line marks fission cutoff angular momentum $69\hbar$ [4,19]. The ratios of major to minor axis according to the RLDM and corresponding to set 1 are also shown.

side. A similar, but smaller deviation, is observed for deuterons and tritons. No significant variations of the fission cross sections are obtained ($\sigma_{fiss}=347$ mb) with respect to OM (set 2) transmission coefficient calculations.

The results obtained using transmission coefficients from fusion systematics (FS) [14], keeping set 2 for the phase space parameters, are shown in Fig. 4 for protons and alpha particles. The Hill-Wheeler [28] expression has been used with barrier curvatures $\hbar\omega=4.0$ and 3.0 MeV for ^{4}He and ^{1}H, respectively, and with fusion s-wave barriers [14]. A comparison between the data and results obtained using OM and IWBCM transmission coefficients is also presented in the figure. We have not included deuterons and tritons in the calculations, as no transmission coefficients from fusion systematics are available for these particles. A slightly lower fission cross section was obtained ($\sigma_{fiss}=297$ mb). FS transmission coefficients provide a ^{1}H energy spectrum significantly harder than that obtained with the other sets of transmission coefficients, indicating a larger discrepancy between data and calculations, while, for ^{4}He, FS and IWBCM transmission coefficients provide essentially equivalent results, as far as the low-energy side is concerned. It must be pointed out that we are faced with a high degree of uncertainty for the barrier curvature in the case of protons [14]. It is well known that smaller values of barrier curvature, as suggested in Ref. [14], make larger the discrepancy with the data. Such changes in the proton spectra modify the ^{4}He spectra through the competition [12].

B. Cross sections

The comparison between ^{1,2,3}H and ^{4}He measured cross sections and CASCADE predictions is shown in Table II. The corresponding values of the fission cross section are also reported. Both sets 1 and 2 provide a reasonable agreement with the measured value of the ^{1}H cross section. For ^{4}He, set 2 underpredicts the measured value. As already found by Fornal *et al.* [4], the use of OM transmission coefficients, of a lowered yrast line and fission parameters from Ref. [20] provides a ^{4}He cross section lower than the measured one. Finally, ^{2,3}H cross sections are largely overestimated by both calculations.

The IWBCM provides a reasonable agreement for all the particles except for ^{4}He, whose cross section is largely underestimated. Fusion systematics transmission coefficients provide cross sections very close to those obtained with the OM set 2 of parameters; variations of only a few percent are obtained with the curvature going form 1 to 4 MeV for protons.

To summarize, IWBCM transmission coefficients provide reasonable agreement with ^{1,2,3}H cross sections, but they underestimate the ^{4}He cross section and the low-energy side of ^{1,2,3}H and ^{4}He energy spectra. On the oth-

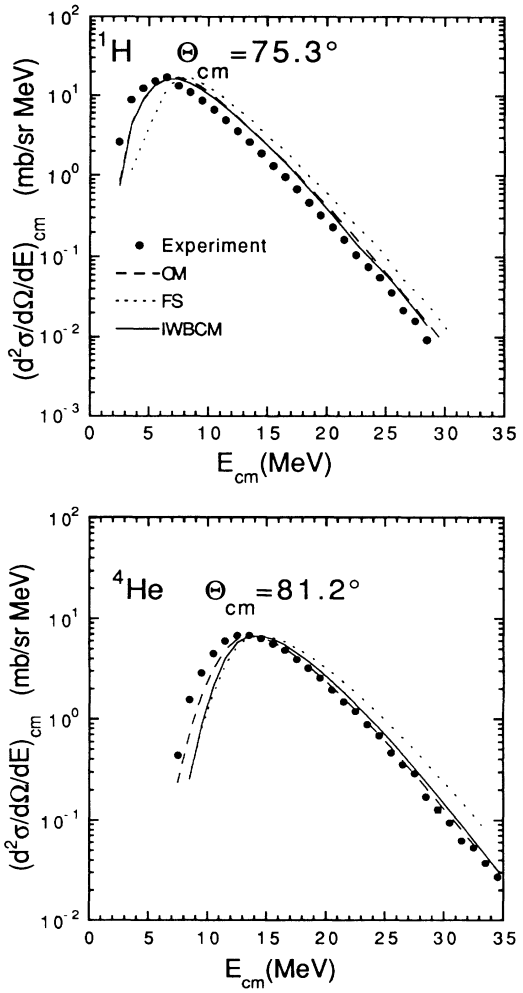

FIG. 4. Measured ^{1}H and ^{4}He energy spectra compared with CASCADE calculations using optical model (OM), fusion systematics (FS), and ingoing-wave boundary-condition model (IWBCM) transmission coefficients.

TABLE II. Comparison between experimental and calculated cross sections of evaporated ^{1,2,3}H and ^{4}He particles in the reaction of 180-MeV ^{32}S+^{64}Ni.

		^{1}H	^{2}H	^{3}H	^{4}He	σ_f
Experiment		1860±279	87±17	16±3	1405±211	200[a]
OM	set 1	1821	181	31	1399	108
OM	set 2	1809	168	26	928	341
FS	set 2	1978			820	297
IWBCM	set 2	1990	96	14	639	347
IWBCM	$(1.15r_0)$	1963	102	16	1411	236

[a]Fission cross section (σ_f) is estimated from a ^{35}Cl+^{64}Ni reaction [20].

er hand, OM transmission coefficients provide shapes of energy spectra relatively close to those obtained with IWBCM transmission coefficients, but they overestimate by a factor of ≈ 2 the ^{2,3}H yields. Finally FS transmission coefficients reproduce the ^{1}H cross section, but they underestimate the ^{4}He one at the same time that the calculated spectra are significantly more energetic than the measured ones. Considering that we may improve the agreement between the data and model by lowering the emission barriers, IWBCM transmission coefficients appear to be the best candidate to provide a good overall description of the data. In fact, both the deviations in the energy spectrum and cross section in the case of ^{4}He can be eliminated by lowering the emission barrier, provided that a reasonable value for fission cross section is obtained. Nevertheless, the need of barrier reduction, required by the ^{1}H energy spectrum, is at odds with the corresponding yield, as this latter is already well reproduced by this set of transmission coefficients. Therefore we may not be able to reproduce both the shape of the energy spectrum and the cross section of protons, this expectation being true independent from the kind of transmission coefficients. In order to gain insight on this point, calculations with reduced barriers in the IWBCM transmission coefficients have been carried out. The results are presented in the next paragraph.

C. Barrier reductions

We intend here to investigate if we can obtain a satisfactory description of the shapes of the spectra and cross sections of all four particles, reducing the emission barriers in the evaporation model. To pursue this objective, we have performed calculations, increasing the radii of the IWBCM potential for ^{1,2,3}H and ^{4}He, in order to reproduce the low-energy side of the energy spectra and, in the case of ^{4}He, the yield. First, we have performed calculations, increasing the radius for one particle at the time, in order to evaluate the sensitivity of the result. Then a complete calculation, including reduced barriers for all the particles, has been carried out.

The calculated spectra obtained by increasing the radius by a factor $f = 1.15$ for all the particles are shown in Fig. 5. The corresponding cross sections are given in

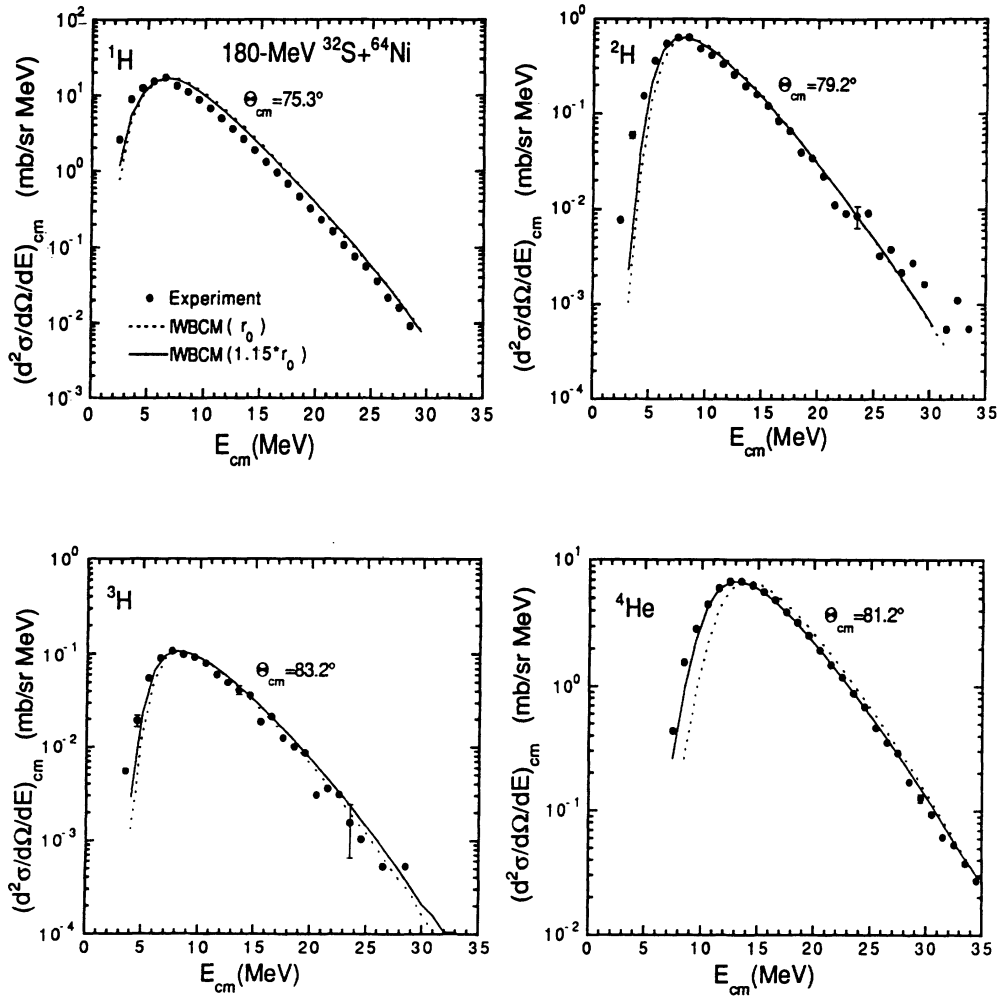

FIG. 5. Comparison between ^{1,2,3}H and ^{4}He energy spectra and CASCADE calculations using the ingoing-wave boundary-condition model (IWBCM) and the IWBCM with increased radii of the potential.

Table II. The shapes of the energy spectra and the multiplicities of all the particles are well reproduced, except the proton spectrum, which is not sensitive to this change.

On the contrary, we cannot obtain a similar agreement using OM transmission coefficients, no matter how we increase the potential radius. In particular, reducing only the ^{4}He barrier by a small amount (corresponding to $f=1.08$), we can obtain good agreement for the alpha cross section without changing significantly the cross sections for the other particles (less than 10%), leaving a large disagreement for ^{2}H and ^{3}H. On the other hand, a reduction in the ^{2}H and ^{3}H barriers would enhance the disagreement with the data. Finally, the proton spectrum is not sensitive to barrier reductions, leaving the same discrepancy observed using the IWBCM transmission coefficients.

In order to observe variations in the proton spectrum, using both IWBCM and OM transmission coefficients, we have to increase the radius of the proton potential by a factor of 1.5. This choice already provides, in the IWBCM case, a value for the proton cross section ($\sigma_p=3154$ mb) and for the alpha one ($\sigma_\alpha=934$ mb) much larger and smaller than the measured ones, respectively. Deuteron and triton yields are not much affected, with values still within the experimental uncertainties.

The agreement found with the IWBCM is not much affected by the change of the other particles yields. In fact, the relatively small dependence of ^{2,3}H yields from the proton yields is not surprising because such a dependence is related to the total decay width. A significant change in the proton decay width produces a small change in the total decay width.

The possibility of reproducing the ^{1}H spectral shape and cross section, at the same time modeling the phase space and adopting reduced barriers in the transmission coefficients, has been ruled out by several trials. Different values for the deformability parameters, for the moment of inertia of the residual nucleus, for the level density parameter, for the interpolation range between the low-energy and the liquid drop regions, and, finally, different options for the liquid drop formula, were used.

D. *s*-wave emission barriers

First-step emission *s*-wave barriers for the IWBCM transmission coefficients are presented in Table III, as well as the reduced *s*-wave barriers needed to obtain the energy spectra shown in Fig. 5. The corresponding barriers for OM and FS transmission coefficients and the reduced barriers derived from systematics [1] are also reported for comparison. It is interesting to note that *s*-wave barrier values are equal for the sets of transmission coefficients used, except for protons. For the latter the transparency effects, present in the OM, make this comparison not straightforward. Furthermore, the found barrier reduction for ^{4}He is in good agreement with that obtained from systematics [1]. For protons, our result is consistent with that found in Ref. [1], as a barrier value much lower than that reported in Table III is needed to reproduce the proton spectrum.

IV. DISCUSSION

There are two main results from this work which deserve to be discussed. The first one is the reasonable overall agreement obtained with the IWBCM transmission coefficients in the evaporation model, with particular interest in the ^{2,3}H yields. The second one concerns the failure of the model in reproducing ^{1}H data.

A. Transmission coefficients and their effects on the statistical model predictions

We intend to discuss here the nature of the transmission coefficients used and how the differences between them determine different predictions of the model about cross sections and energy spectra. We compare in Fig. 6 the transmission coefficients derived from the optical model and from the ingoing-wave boundary-condition model for a first-step emission.

For protons, the values of the IWBCM transmission coefficients approach unity for large energy values, while those of the OM ones saturate at $T_L\simeq 0.8$. This behavior, which is related to the transparency effect in the optical potential, arises from the rather great probability that an incident proton will both penetrate the barrier to enter and subsequently reemerge from the target. A similar but much smaller effect is observed for the heavier particles. A second difference between the two sets of transmission coefficients is given by the larger values of the OM transmission coefficients, compared with the IWBCM ones, for a given energy and for high values of orbital angular momenta. As already pointed out in Ref. [15], this difference is due to the treatment of absorption. The radial tail of the imaginary potential causes reactive

TABLE III. Effective *s*-wave barriers (defined by the energies of $T_{l=0}=0.5$) for the evaporation of ^{1,2,3}H and ^{4}He from the composite system ^{96}Ru. Values in parentheses indicate the percent reduction in barriers for the IWBCM corresponding to the energy spectra shown in Fig. 5 with solid lines.

Particle	OM	FS	IWBCM	Reduced IWBCM	Reduced barriers[a]
^{1}H	8.6	6.7	6.7	6.1 (9%)	3.8
^{2}H	6.1		6.1	5.7 (7%)	
^{3}H	5.9		6.0	5.6 (7%)	
^{4}He	12.1	12.1	12.1	10.8 (11%)	10.7

[a]From Ref. [1].

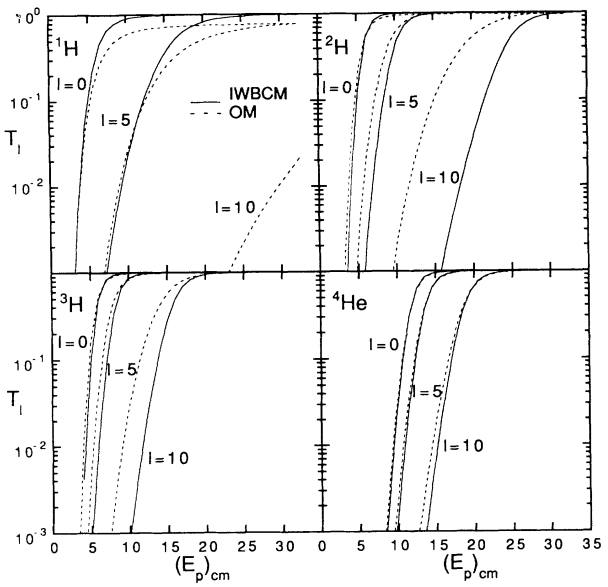

FIG. 6. Comparison between ^{1,2,3}H and ^{4}He optical model transmission coefficients and those derived from the ingoing-wave boundary-condition model for a first-step emission from the composite system ^{96}Ru.

scattering in peripheral collisions that do not penetrate the real barrier.

For ^{2,3}H which are emitted in the first steps of the evaporative chain, the behavior of the transmission coefficients shown in Fig. 6 reflects well most of the differences found in the calculated cross sections. For ^{4}He, the two sets of transmission coefficients are almost equivalent: The difference in the calculated cross sections (Table II) is determined by the slightly smaller values of the IWBCM with respect to OM transmission coefficients at relatively high values of L. For ^{1}H, in spite of the differences in the transmission coefficients, the two sets provide similar values of cross sections. Here the transparency effect, which lowers the OM transmission coefficients, increasing the energy, at a fixed L, is compensated by the effect of the absorption outside the well.

Concerning the spectral shapes, most of the differences resulting from the use of OM and IWBCM transmission coefficients can be understood from the comparison shown in Fig. 6.

For ^{2}H and ^{3}H, IWBCM transmission coefficients reduce the widths of the energy spectra (Fig. 2). This produces a better agreement at the high-energy side, while at low energy the calculation underestimates the data more than the OM transmission coefficients. In particular, at energies below 10 MeV, where the transmission coefficients play an important role, only L values up to $(5-6)\hbar$ contribute significantly to the spectrum. For these latter, the OM provides transmission coefficients larger than those obtained with the IWBCM, leading to larger values of the cross section in the spectrum. At high energies, although the difference between the coefficients becomes very large, the effect on the spectrum is attenuated by the level density, which plays the leading role.

Similar considerations can be done for the low-energy side of the ^{4}He spectrum, while at high energies the difference is very small.

Finally, the proton spectrum is not sensitive to the sets of transmission coefficients. The situation is more complicated for protons, not only because the emission of this particle takes place over many steps of the evaporative chain, but also because the interplay between transparency effect and absorption outside the well is more complex than for the other particles.

We compare, in Fig. 7, IWBCM and FS transmission coefficients. For ^{4}He, the two sets are essentially equivalent. For protons, at energies lower than 5–6 MeV, FS transmission coefficients are significantly smaller than IWBCM ones. This is the reason for the low-energy missing protons using FS transmission coefficients. At the same time, the larger values of FS transmission coefficients at high energy, for each L, compared with the IWBCM, enhance proton emission at the high-energy side of the spectrum, as we can see in Fig. 4. We should remark here that the Hill-Wheeler expression may not be appropriate for protons. As indicated in Ref. [14], the excitation function of the inverse process is not well reproduced using this expression in the barrier penetration model. Nevertheless, in some cases, the Hill-Wheeler expression appears to work reasonably well,

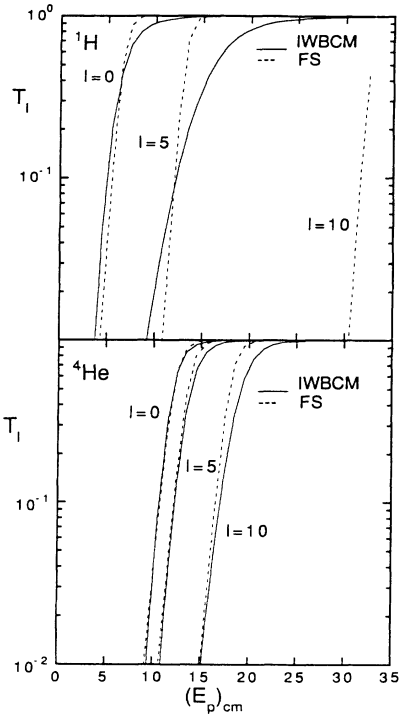

FIG. 7. Comparison between ^{1}H and ^{4}He Hill-Wheeler [28] transmission coefficients matched with fusion systematics [14] and those derived from the ingoing-wave boundary-condition model for a first-step emission from the composite system ^{96}Ru. In the Hill-Wheeler expression, barrier curvature ($\hbar\omega$) values of 3 and 4 MeV have been used for ^{1}H and ^{4}He, respectively.

although barrier lowerings are still observed [1,33].

Taking into account the physical description provided by the IWBCM together with the better overall agreement obtained, we can conclude that these transmission coefficients are more appropriate for the description of particle evaporation in this system. A similar comparison, carried out through a systematic analysis of the yields of ^{2,3}H, emitted for a certain number of composite nuclei at excitation energies of ≈ 100 MeV, has given similar results [34].

B. Deviations from the predictions of the evaporation model

For proton spectra we have found that the deviations are independent from the phase space parameters and from the set of transmission coefficients used. This discrepancy leaves an open question about the statistical model and on our conclusions about the transmission coefficients. As indicated in recent investigations [1,6,8,9], the protons seem to play an important role in the understanding of possible novel features in the evaporation process. Descriptions in terms of emitter deformation and/or dynamical effects may be called upon to explain the experimental data. It would be interesting to compare our results with those obtained including dynamical effects in the statistical model. If dynamical effects, necessary to explain proton spectra, would change significantly the emission of the other light particles, the conclusion about the transmission coefficients should be revised.

ACKNOWLEDGMENTS

The authors wish to thank Professor M. Kaplan and Professor J. M. Alexander for valuable discussions and suggestions. We thank the technicians F. Manna and A. Parmentola for the excellent support provided to the experiment.

[1] W. E. Parker, M. Kaplan, D. J. Moses, G. La Rana, D. Logan, R. Lacey, J. M. Alexander, D. M. de Castro Rizzo, P. DeYoung, and R. J. Welberry, Phys. Rev. C **44**, 774 (1991).

[2] Z. Majka, M. E. Brandan, D. Fabris, K. Hagel, A. Menchaca-Rocha, J. B. Natowitz, G. Nebbia, G. Prete, B. Sterling, and G. Viesti, Phys. Rev. C **35**, 2125 (1987).

[3] R. K. Choudhury, P. L. Gonthier, K. Hagel, M. N. Namboodiri, J. B. Natowitz, L. Adler, S. Simon, S. Kniffen, and G. Berkowitz, Phys. Lett. **143B**, 74 (1984).

[4] B. Fornal, F. Gramegna, G. Prete, G. Nebbia, R. Smith, G. D'Erasmo, L. Fiore, A. Pantaleo, G. Viesti, P. Blasi, F. Lucarelli, I. Iori, and A. Moroni, Phys. Rev. C **41**, 127 (1990).

[5] B. Fornal, G. Viesti, G. Nebbia, G. Prete, and J. B. Natowitz, Phys. Rev. C **40**, 664 (1989).

[6] G. La Rana, D. J. Moses, W. E. Parker, M. Kaplan, D. Logan, R. Lacey, J. M. Alexander, and R. J. Welberry, Phys. Rev. C **35**, 373 (1987).

[7] G. La Rana, R. Moro, A. Brondi, P. Cuzzocrea, A. D'Onofrio, E. Perillo, M. Romano, F. Terrasi, and E. Vardaci, Phys. Rev. C **37**, 1920 (1988).

[8] R. Lacey, N. N. Ajitanand, J. M. Alexander, D. M. deCastro Rizzo, P. DeYoung, M. Kaplan, L. Kowalski, G. La Rana, D. Logan, D. J. Moses, W. E. Parker, G. F. Peaslee, and L. C. Vaz, Phys. Lett. B **191**, 253 (1987).

[9] G. Bozzolo, O. Civitarese, and J. P. Vary, Phys. Lett. B **219**, 161 (1989).

[10] I. M. Govil, J. R. Huizenga, W. U. Schroder, and J. Toke, Phys. Lett. B **197**, 515 (1987).

[11] N. G. Nicolis and D. G. Sarantites, Phys. Rev. C **40**, 2422 (1989).

[12] G. La Rana, R. Moro, A. Brondi, P. Cuzzocrea, A. D'Onofrio, E. Perillo, M. Romano, and F. Terrasi, Phys. Rev. C **40**, 2425 (1989).

[13] M. A. McMahan and J. M. Alexander, Phys. Rev. C **21**, 1261 (1980).

[14] L. C. Vaz and J. M. Alexander, Z. Phys. A **318**, 231 (1984).

[15] J. M. Alexander, M. T. Magda, and S. Landowne, Phys. Rev. C **42**, 1092 (1990).

[16] A. Chbihi, L. G. Sobotka, Z. Majka, D. G. Sarantites, D. W. Stracener, V. Abenante, T. M. Semkow, N. G. Nicolis, D. C. Hensley, J. R. Beene, and M. L. Halbert, Phys. Rev. C **43**, 652 (1991); A. Chbihi, L. G. Sobotka, N. G. Nicolis, D. G. Sarantites, D. W. Stracener, Z. Majka, D. C. Hensley, J. R. Beene, and M. L. Halbert, *ibid.* **43**, 666 (1991).

[17] N. G. Nicolis, D. G. Sarantites, L. G. Sobotka, and R. J. Charity, Phys. Rev. C **45**, 2393 (1992).

[18] N. N. Ajitanand, R. Lacey, G. F. Peaslee, E. Duek, and J. M. Alexander, Nucl. Instrum. Methods Phys. Res. A **243**, 111 (1986).

[19] F. Puhlhofer, Nucl. Phys. **A280**, 267 (1977).

[20] B. Sikora, W. Scobel, M. Beckerman, J. Bisplinghoff, and M. Blann, Phys. Rev. C **25**, 1446 (1982).

[21] S. Cohen, F. Plasil, and W. J. Swiatecki, Ann. Phys. (N.Y.) **82**, 557 (1974).

[22] D. Wilmore and P. E. Hodgson, Nucl. Phys. **55**, 673 (1964).

[23] F. G. Perey, Phys. Rev. **131**, 745 (1963).

[24] J. M. Lohr and W. Naeberly, Nucl. Phys. **A232**, 381 (1974).

[25] F. D. Becchetti, Jr. and G. W. Greenlees, in *Polarization Phenomena in Nuclear Reactions,* edited by H. H. Barshall and W. Haeberli (The University of Wisconsin Press, Madison, Wisconsin, 1971), p. 682.

[26] J. R. Huizenga and G. Igo, Nucl. Phys. **29**, 462 (1961).

[27] S. Landowne and S. C. Pieper, Phys. Rev. C **29**, 1352 (1984).

[28] D. L. Hill and J. A. Wheeler, Phys. Rev. **89**, 1102 (1953).

[29] W. D. Meyers and W. J. Swiatecki, Ark. Fys. **36**, 343 (1967).

[30] W. Dilg, W. Schantl, H. Vonach, and M. Uhl, Nucl. Phys. **A217**, 269 (1973).

[31] D. W. Lang, Nucl. Phys. **77**, 545 (1966).

[32] W. D. Meyers and W. J. Swiatecki, Nucl. Phys. **81**, 1 (1966).

[33] U. Gollerthan, T. Brohm, H.-G. Clerc, E. Hanelt, M. Horz, W. Morawek, W. Schwab, K.-H. Schmidt, F. P. Hessberger, G. Munzenberg, V. Ninov, R. S. Simon, J. P. Dufour, and M. Montoya, Z. Phys. A **338**, 51 (1991).

[34] M. Kildir, G. La Rana, R. Moro, A. Brondi, A. D'Onofrio, E. Perillo, M. Romano, F. Terrasi, E. Vardaci, G. Nebbia, G. Viesti, and G. Prete (unpublished).